

# We are IntechOpen, the world's leading publisher of Open Access books Built by scientists, for scientists

6,900

Open access books available

185,000

International authors and editors

200M

Downloads

Our authors are among the

154

Countries delivered to

TOP 1%

most cited scientists

12.2%

Contributors from top 500 universities



WEB OF SCIENCE™

Selection of our books indexed in the Book Citation Index  
in Web of Science™ Core Collection (BKCI)

Interested in publishing with us?  
Contact [book.department@intechopen.com](mailto:book.department@intechopen.com)

Numbers displayed above are based on latest data collected.  
For more information visit [www.intechopen.com](http://www.intechopen.com)



## Biomimetic Topography: Bioinspired Cell Culture Substrates and Scaffolds

Lin Wang and Rebecca L. Carrier  
Northeastern University  
USA

### 1. Introduction

*In vivo*, cells are surrounded by 3D extracellular matrix (ECM), which supports and guides cells. Topologically, ECM is comprised of a heterogeneous mixture of pores, ridges and fibers which have sizes in the nanometer range. ECM structures with nanoscale topography are often folded or bended into secondary microscale topography, and even mesoscale tertiary topography. For example, ECM of small intestine folds into a 3D surface comprising three length scales of topography: the centimeter scale mucosal folds, sub-millimeter scale villi and crypts, and nanometer scale topography which is created by ECM proteins, such as collagen, laminin, and fibronectin. Techniques such as photolithography, two-photon polymerization, electrospinning, and chemical vapor deposition have been utilized to recreate certain ECM topographical features at specific length scales or exactly replicate complex and hierarchical topography *in vitro*. Various *in vitro* tests have proven that mammalian cells respond to biomimetic topographical cues ranging from mesoscale to nanometer scale (Bettinger et al., 2009, Discher et al., 2005, Flemming et al., 1999). One of the most well-known effects is contact guidance, in which cells respond to groove and ridge topography by simultaneously aligning and elongating in the direction of the groove axis (Teixeira et al., 2003, Webb et al., 1995, Wood, 1988). It has also been noted that cell response to biomimetic topography *in vitro* depends on cell type, feature size, shape, geometry, and physical and chemical properties of the substrate. Questions such as whether cells respond to topographical features using the same sensory system as that used for cell-matrix adhesion; whether the size and the shape of scaffold topography may affect cell response or cell-cell interaction; whether the ECM topology plays a role in coordinating tissue function at a molecular level, other than providing a physical barrier or a support; and whether ECM topography affects local protein concentration and adhesion of cell binding proteins, are beginning to be answered.

This chapter begins by considering topography of native ECM of different tissues, and methods and materials utilized in the literature to recreate biomimetic topography on cell culture substrates and scaffolds. The influence of nanometer to sub-millimeter shape and topography on mammalian cell morphology, migration, adhesion, proliferation, and differentiation are then reviewed; and finally the mechanisms by which biomimetic topography affects cell behavior are discussed.

## 2. Topography of native extracellular matrix

The native ECM is comprised of fibrous collagen, hyaluronic acid, proteoglycans, laminin, fibronectin etc., which provide chemical, mechanical, and topographical cues to influence cell behavior. Extensive research has been carried out to study the effects of ECM chemistry and mechanics on cell and tissue functions. For example, ECM regulates cell adhesion through ligand binding to some specific region (e.g. RGD) of ECM molecules (Hay, 1991); the strength of integrin-ligand binding is affected by matrix rigidity (Choquet et al., 1997). Topologically, ECM is comprised of a heterogeneous mixture of pores, ridges and fibers which have sizes in the nanometer range (Flemming et al., 1999). The ECM sheet with nanoscale topography is often folded or bended to create secondary microscale topography, and even a mesoscale tertiary topography. Hierarchical organization over different length scales of topography is observed in many tissues. For example, scanning electron microscope (SEM) examination of human thick skin dermis ECM reveals surface topography over different length scales (Kawabe et al., 1985). The primary topography is composed of millimeter scale alternating wide and narrow grooves called primary and secondary grooves, respectively. Sweat glands reside in primary grooves, and topographically the bottoms of primary grooves are smoother than the bottoms of secondary grooves. The millimeter size ridges are comprised of submillimeter to several hundred micron finger-like projections: dermal papillae. The surface of each dermal papillae is covered by folds and pores approximately 10 microns in dimension. The interstitial space is composed of dermal collagen fibrils 60-70 nm in diameter forming a loose honey comb like network. The hierarchical topographies are also seen in the structure of bone, where bone structure is comprised of concentric cylinders 100 – 500  $\mu\text{m}$  in diameter called osteons, which are made of 10 – 50  $\mu\text{m}$  long collagen fibers (Stevens&George, 2005). The surface topography of pig small intestinal extracellular matrix, which we are working to replicate in our lab, also reveals a series of structures over different length scales (**Figure 1**). There are finger-like projections (villi) of millimeter to 400 – 500  $\mu\text{m}$  scale, and well-like invaginations (crypts) 100 – 200  $\mu\text{m}$  in scale. The surface of the basement membrane of villi is covered by 1 – 5  $\mu\text{m}$  pores, and approximately 50 nm thick collagen fibers. These observations agree with what has been reported in the literature (Takahashi-Iwanaga et al., 1999, Takeuchi&Gonda, 2004). On the surface of rat small intestine ECM, the majority of micron-size pores are located at the upper three fourths of the villi. The pore diameter is larger in the upper villi than in the lower villi.

The basement membrane is a specialized ECM, which is usually found in direct contact with the basolateral side of epithelium, endothelium, peripheral nerve axons, fat cells and muscle cells (Merker, 1994, Yurchenco&Schittny, 1990). The surface of native tissue basement membrane presents a rich nanoscale topography consisting of pores, fibers, and elevations, which gives each tissue its unique function. Abrams *et al.* (Abrams et al., 2000) examined nanoscale topography of the basement membrane underlying the anterior corneal epithelium of the macaque by SEM, transmission electron microscopy (TEM) and atomic force microscopy (AFM) (**Figure 2**). The average mean surface roughness of monkey corneal epithelium basement membrane was between 147 and 194 nm. The surface of basement membrane is dominated by fibers with mean diameters around  $77\pm44$  nm and pores with diameters around  $72\pm40$  nm. The porosity of basement membrane is approximately 15% of the total surface area. The porous structure was postulated to have a filtering function, as well as provide conduits for penetration of subepithelial nerves into the epithelial layer.

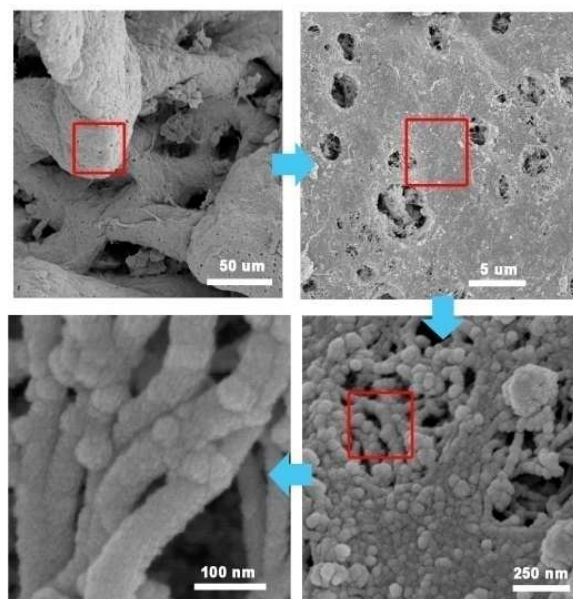


Fig. 1. Hierarchical organization of different length scale structures on the surface of pig small intestinal extracellular matrix, after removal of epithelium.

Hironaka *et al.* (Hironaka et al., 1993) examined the morphologic characteristics of renal basement membranes (i.e. glomerular, tubular, Bowman's capsule, peritubular capillary basement membrane) using ultrahigh resolution SEM (**Figure 2**). It was demonstrated that morphologically, renal basement membrane was composed of 6 - 7 nm wide fibrils forming polygonal meshwork structures with pores ranging from 4 - 50 nm. The observation of bladder basement membrane ultrastructures showed that the average thickness of bladder basement membrane is 178 nm with mean fiber diameters around 52 nm. The porous features were also found in bladder basement membrane, with mean pore diameter around 82 nm and mean inter pore distance (center to center) 127 nm (Abrams et al., 2003). In our study, it was observed that nanoscale topography of pig intestinal basement membrane was also comprised of pores and fibers (**Figure 2**) (Wang et al., 2010). Interestingly, unlike corneal, renal, and bladder basement membrane, which often have pores around 100 nm in diameter, intestinal basement membrane has pores larger than 500 nm. Other than being perforated with 1 - 5  $\mu\text{m}$  pores, the rest of the intestinal basement membrane surface is occupied by more densely packed fibers compared with corneal, renal, or Matrigel™ surfaces.

In general, ECM of native tissues possesses rich topography over broad size ranges. Length scales of topography usually range from centimeter to nanometer, and surface features of extracellular matrix often follows a fractal organization, consisting of structures comprised of repeating units throughout different levels of magnification. Most native ECM has "subunit" topography, such as papillae at the surface of dermal ECM; osteons in bone tissue; and villi and crypts at the surface of small intestine ECM, whose sizes are around 1 mm to 100  $\mu\text{m}$ . The ECM surface also exhibits rich nanotopography (nanopores, and interwoven fibrils), created by ECM proteins. The size, density, and distribution of fibrils and pores are highly dependent on the source tissue (**Figure 2**) (Sniadecki et al., 2006, Stevens&George, 2005). Information on native ECM topography provides a rational basis for surface feature design of biomimetic tissue culture substrates or scaffolds.



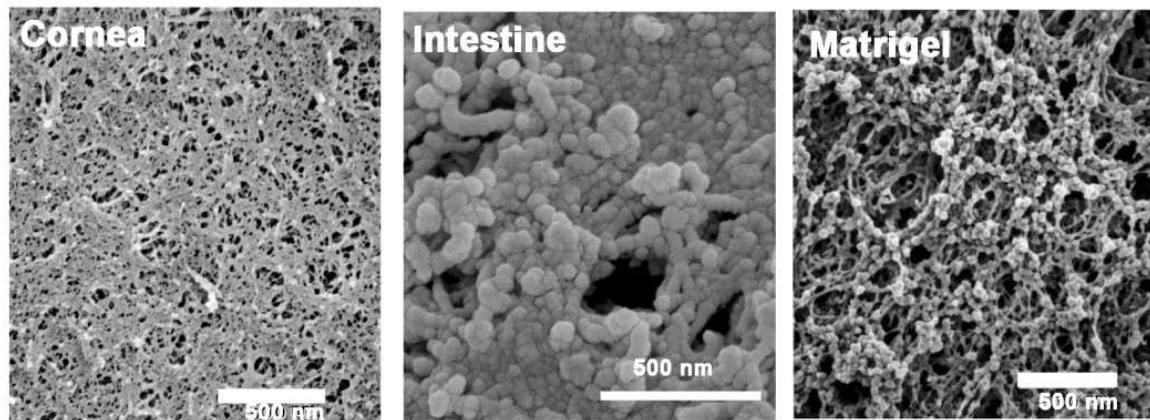


Fig. 2. Nanoscale topography and structure of basement membranes of anterior corneal epithelium (adapted with permission from Abrams et al., 2000), small intestine, and Matrigel (adapted with permission from Abrams et al., 2000)

### 3. Patterned cell culture substrates: fabrication methods & materials

Various methods and materials have been utilized to create 3D cell culture substrates and tissue culture scaffolds. Depending on desired 3D features as well as chemical and mechanical properties of the scaffold, a specific fabrication strategy can be selected. There are four main categories of methods reported in the literature for fabrication of a 3D cell culture substrate or scaffold: (1) methods resulting in precisely designed regular surface topographies or 3D features; (2) methods resulting in irregular topographies, such as 3D fibrils, pores, or simple increased surface nanoscale roughness; (3) methods aiming for exact replication of 3D feature of native tissue; (4) methods based on naturally derived biopolymer gels or decellularized ECM.

Micro- and nanofabrication methods, such as photolithography, electron-beam lithography, two-photon polymerization, microcontact printing and etching, have often been employed to produce surface features with controlled dimensions and specific shapes (reviewed by (Bettinger et al., 2009)). Among these techniques, photolithography is the most popular approach and is often used to generate regular surface features, such as grooves, posts, and pits. Photolithography, and other micro- nanofabrication techniques are typically fine-tuned for silicon, silicon oxide, polycrystalline silicon, and other inorganic systems such as titanium. Therefore, either these inorganic materials, such as silicon or titanium, or organic polymers replicas of inorganic master molds have been utilized as cell culture substrates to study the effect of topography on cell behavior (Reviewed by (Bettinger et al., 2009)). Organic polymers used in this manner include poly (dimethylsiloxane), polystyrene, poly(methyl methacrylate), polycarbonate, and poly(ethylene glycol), as well as biodegradable polymers such as poly ( $\epsilon$ -caprolactone), poly(L-lactic acid), poly(glycolic acid), and poly(L-lactic-co-glycolic acid). Some more recently developed techniques, such as multiphoton lithography, are capable of fabricating much more complex 3D topographies than simple groove, post or pit arrays. For example, it was reported that layer-by-layer stereolithography was able to create free-form complicated 3D constructs: a layer of 400 mg/ml bovine serum albumin (BSA) was deposited and photocrosslinked by exposed to patterned UV light, and repeated many times to incrementally build a 3D structure. The

resolution of multiphoton lithography is around 0.1 – 0.5  $\mu\text{m}$ , which is in a similar range as soft lithography (Nielson et al., 2009).

Electrospinning processes are able to create 3D scaffolds comprised of non-woven fibrous networks with fiber diameters ranging from tens of nanometers to microns (Liang et al., 2007). Synthetic polymers, such as polyamides, polylactides, cellulose derivatives, and water soluble polyethyleneoxide; natural polymers, such as collagen (type I, II, III), elastin, silk fibrin, and chitosan; and copolymers of either synthetic or natural polymers can be adapted to electrospinning processes (Liang et al., 2007). Fiber diameter, morphology, porosity, and biological properties of electrospun scaffolds can be modified via copolymerization or adjusting electrospinning conditions. Traditional electrospinning processes are only capable of creating nanofibers with random orientations; however, perfectly aligned fiber scaffolds can be obtained via modification of fiber collection methods (Liang et al., 2007). Techniques such as fiber bonding (unwoven mesh), solvent casting/particulate leaching, gas foaming and phase separation/emulsification have been utilized to produce porous scaffolds (Mikos&Temenoff, 2000). Porous structure allows cells to penetrate into the scaffold and facilitates nutrient and waste exchange of cells located deep inside of constructs. One fiber bonding technique creates porous constructs by soaking polymer (e.g., PGA) fibers in another polymer (e.g., PLLA) solution, evaporating the solvent, heating the polymer mixture above the melting point, and finally removing one polymer through dissolving in an organic solution (e.g. methylene chloride). This method can result in a polymer (PGA) foam with porosities as high as  $\sim 80\%$  (Mikos et al., 1993a). The solvent casting/particulate leaching process involves the use of a water soluble porogen. First polymer (e.g., PLLA, PLGA) is dissolved in an organic solvent (e.g., methylene chloride) and then mixed with porogen (e.g. NaCl). After evaporating the solvent, the salt crystals inside the polymer/salt composite are removed by leaching in water, resulting in a porous polymer scaffold. The pore size and pore density can be controlled by the amount and size of salt crystal (Mikos et al., 1993b). The gas foaming method utilizes gas as a porogen, where a polymer (e.g., PGA, PLLA, PLGA) is exposed to high pressure gas (e.g.,  $\text{CO}_2$ ) for a long period of time (e.g., 72 h), and then the pressure is rapidly reduced to atmospheric pressure, resulting in a polymer scaffold with porosities up to 93% (Mooney et al., 1996). Phase separation/emulsification methods create porous scaffolds based on the concepts of phase separation rather than incorporation of a porogen (Mikos&Temenoff, 2000). For example, Whang *et al.* (Whang et al., 1995) dissolved PLGA in methylene chloride and then added water into the PLGA solution to form an emulsion. The mixture was cast into a mold and freeze-dried to remove water and methylene chloride, resulting in a scaffold with high porosities (up to 95%) but relatively small pore size ( $< 40 \mu\text{m}$ ). In addition to generating fibrillous or porous scaffolds utilizing techniques such as electrospinning, particulate leaching, and gas foaming; irregular surface topography can also be fabricated by abrading. For example, Au *et al.* (Au et al., 2007) created rough polyvinyl carbonate surface by abrading the surface with 1 – 80  $\mu\text{m}$  grain size lapping paper. The resulting surface had V-shaped abrasions with peak to peak widths from 3 – 13  $\mu\text{m}$ , and depths from 140 – 700 nm.

Other methods, such as chemical vapor deposition (CVD), conformal-evaporated-film-by-rotation (CEFR), and deposition in supercritical fluid (Cook et al., 2003, Martín-Palma et al., 2008, Pfluger et al., 2010, Wang et al., 2005) have been utilized to precisely replicate the complex and irregular hierarchical topography from a biological sample over several length scales. Pfluger *et al.* (Pfluger et al., 2010) reported precise replication of the complex

topography of pig small intestinal basement membrane using plasma enhanced CVD of biocompatible polymer: poly(2-hydroxyethyl methacrylate) (pHEMA) (**Figure 3**). A pHEMA film was generated via introducing a mixed vapor of precursor: 2-hydroxyethyl methacrylate, and initiator: tert-butyl peroxide, into a CVD chamber to react with a cross-linker: ethylene glycol diacrylate, when exposed to an Argon plasma. Chemical vapor deposited pHEMA is able to replicate villus (100 – 200  $\mu\text{m}$  in height, 50 – 150  $\mu\text{m}$  in diameter), crypt (20 – 50  $\mu\text{m}$  in diameter), and pore (1 – 5  $\mu\text{m}$  in diameter) structures on the surface of intestinal basement membrane; the thickness of pHEMA coating is around 1  $\mu\text{m}$ . Cook *et al.* (Cook *et al.*, 2003) demonstrated replication of the surface features of butterfly wings using controlled vapor-phase oxidation of silanes. Hydrogen peroxide was evaporated and reacted with gaseous silane creating silica primary clusters, which have extraordinary flow properties and are able to creep into small gaps on the surface of a biological specimen. After the deposition of silica, biological specimen was removed by calcination at 500°C. This method was able to generate a 100 – 150 nm thick replica, which reproduced nanometer scale ( $\sim 500$  nm) features on the surface of a biological sample. Martín-Palma *et al.* (Martín-Palma *et al.*, 2008) created a 0.5 - 1  $\mu\text{m}$  thick chalcogenide glass ( $\text{Ge}_{28}\text{Sb}_{12}\text{Ge}_{60}$ ) replica of fly eyes using oblique angle deposition (OAD) technique while rapidly rotating the specimen (**Figure 3**). The OAD technique is based on directing a vapor towards a substrate with a trajectory of atoms not parallel to the substrate normal. Wang *et al.* (Wang *et al.*, 2005) replicated the surface features of pollen grains and cotton fiber from  $\sim 100$  nm scale upwards (**Figure 3**). The replica was fabricated by dissolving titanium isopropoxide precursor in supercritical  $\text{CO}_2$ , and then depositing on the surface of a biological specimen. The adsorbed precursor then reacted with water molecules and hydroxyl groups on the surface of the biological sample, resulting in the condensation of titanium at the interface. Finally, the biological specimen embedded inside the titanium coating was removed by calcination.

Decellularized tissue and organs are another type of three dimensional scaffold used for tissue engineering/regenerative medicine applications (Gilbert *et al.*, 2006). ECM from a variety of tissues, including heart valves, blood vessels, skin, nerves, skeletal muscle, tendons, ligaments, small intestinal submucosa, urinary bladder, and liver, have been isolated, decellularized, and then used as cell culture scaffolds (reviewed by (Gilbert *et al.*, 2006)). The decellularized ECM often retains biologically functional molecules and three dimensional organization of native ECM, therefore provide a favorable environment for tissue regeneration (Badylak, 2004). Physical, chemical, enzymatic, or combined methods are utilized to decellularize tissue. The physical methods involve agitation, sonication, mechanical massage, pressure, and freezing and thawing. The chemical methods include alkaline and acid treatments, non-ionic detergents (e.g. Triton X-100), ionic detergents (e.g. Triton X-200), Zwitterionic detergents (e.g. CHAPS), tri(n-butyl)phosphate, hypotonic and hypertonic treatment, and chelating agents (e.g. EDTA). Enzymes, such as trypsin, endonucleases, and exonucleases, are also often utilized in decellularization processes (Gilbert *et al.*, 2006). A general approach to decellularization begins with lysis of the cell membrane using physical treatments or incubation with ionic detergent solution, followed by enzymatic treatment to dissociate cellular components from ECM, and removal of cytoplasmic and nuclear cellular components using detergent (Gilbert *et al.*, 2006). Simple hydrogels made of natural polymers, such as ECM components: collagen, elastin, fibrin, hyaluronic acid, and basement membrane extract (e.g. Matrigel<sup>TM</sup>); as well as materials



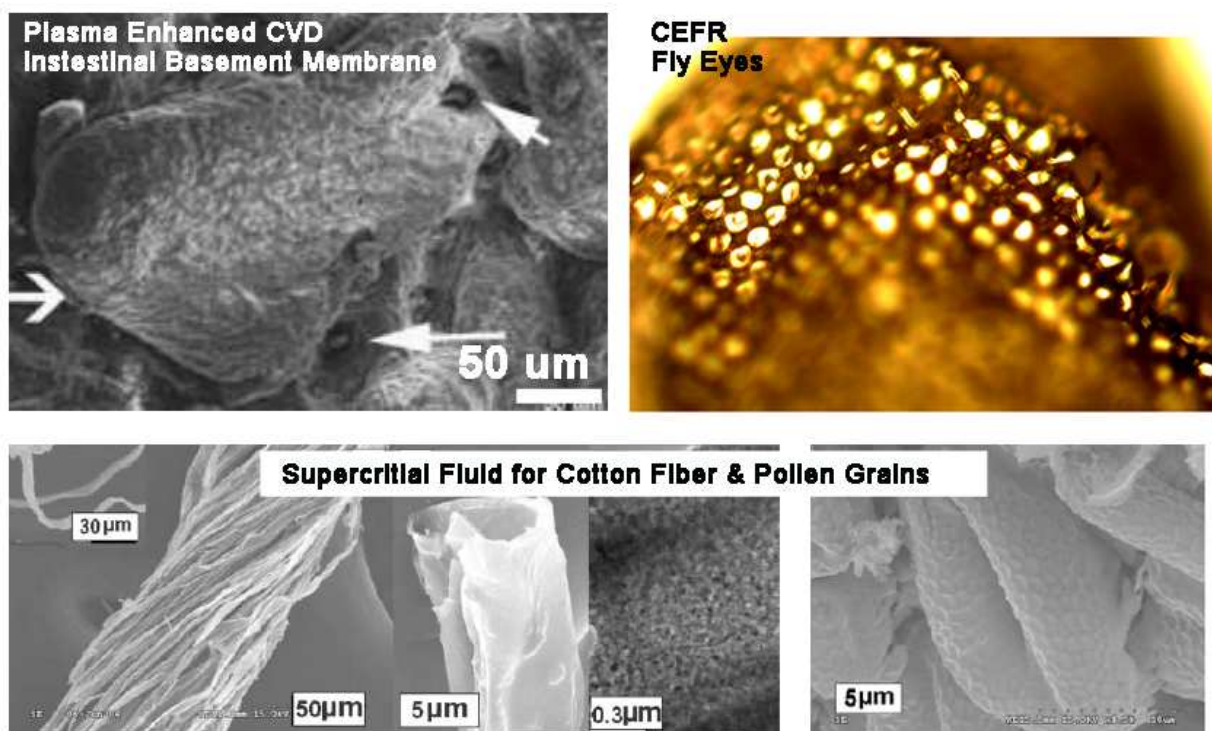


Fig. 3. Precise replication of biological structures: replication of small intestinal basement membrane utilizing plasma enhanced chemical vapor deposition (CVD) of poly(2-hydroxyethyl methacrylate) (adapted with permission from Pfluger et al., 2010); chalcogenide glass ( $\text{Ge}_{28}\text{Sb}_{12}\text{Ge}_{60}$ ) replication of fly eyes by conformal-evaporated-film-by-rotation technique (CEFR) (adapted with permission from Martin-Palma et al., 2008) ; titanium replication of cotton fiber and pollen grains utilizing supercritical  $\text{CO}_2$  (adapted with permission from Wang et al., 2005).

derived from other biological sources: alginate, agarose, chitosan, and silk fibrils, are also utilized for three dimensional cell culture (reviewed by (Lee&Mooney, 2001, Tibbitt&Anseth, 2009)). Collagen is an abundant ECM protein; it forms gels by changing the temperature or pH of its solution (Butcher&Nerem, 2004, Raub et al., 2007); these gels can be further cross-linked by glutaraldehyde or diphenylphosphoryl azide. Gelatin is a derivative of collagen that can also form gels when the temperature of its solution changes. Hyaluronate is one of the ECM glycosaminoglycans; it can form gels by covalently cross-linking with various hydrazide derivatives, and be degraded by hyaluronidase (Pouyani et al., 1994, Vercruysse et al., 1997). Fibrin can be collected from blood, and forms gels by the enzymatic polymerization of fibrinogen at room temperature in the presence of thrombin (Ikari et al., 2000).

Hydrogels can also be formed from synthetic polymers, such as poly(ethylene glycol), poly(vinyl alcohol), poly(2-hydroxy ethyl methacrylate), and polyethylene glycol (PEG). Morphologically, hydrogels are highly porous and have loosely packed fibers. Cells cultured on 3D hydrogel scaffolds can be encapsulated inside the hydrogel scaffold by mixing cell suspension with hydrogel solution and then solidifying, instead of seeding directly on the surface of the hydrogel. The stiffness of hydrogel can be adjusted by varying gel concentration or introducing cross-linking agent.



#### 4. Effect of substrate pattern on cell behavior (morphology, migration, adhesion, proliferation, and differentiation)

Cell shape, migration, and adhesion can be influenced by surface topography of a substrate. Sub-micron to nanometer scale topographies are smaller than the size of a cell and in the similar size range as topography created by ECM proteins, such as collagen, fibronectin, and laminin fibers. This size range of substrate topography may influence cell behavior at the cellular level. Sub-millimeter scale topographies are in the similar range as tissue subunits, such as small intestinal crypt-villus units, osteons of bone, and dermal papillae. As tissue subunits often contain tens to hundreds of cells, sub-millimeter scale topography might influence group cell behavior by affecting cell-cell contact, cell-cell signaling, and other regulation among cells. In the following section, the effect of sub-micron to nanometer scale topography, as well as sub-millimeter scale topography on cell behavior is discussed. Relatively speaking, most studies in the literature pertaining to effect of substrate topography are performed in systems lacking multiple aspects of physiological conditions, utilizing impermeable substrates made of polymer or inorganic materials, such as polydimethylsiloxane, silicon, and titanium oxide. These studies are typically focused on short term effects (culture time equal to or less than 7 days), mostly on cell morphology; the scale of topography is generally limited to cellular to subcellular length scale, and shape of topography is often restricted to simple features such as grooves and ridges. Therefore, more biologically relevant or more biomimetic systems and longer cell culture time might be required to study the effect of substrate topography on cell behavior.

##### 4.1 Cellular and subcellular (ten micron to nanometer) length scale topography

A large body of work has reported that cellular and subcellular length scale topographic features play an important role in affecting cell morphology, migration, and adhesion to substrates. Groove pattern is the most commonly studied pattern type; in general cells have been observed to align along grooves or ridges. Wood *et al.* (Wood, 1988) cultured fin mesenchymal explants on quartz substrates patterned with grooves of 1 – 4  $\mu\text{m}$  width, 1.1  $\mu\text{m}$  depth, and 1 – 4  $\mu\text{m}$  spacing, and found groove topography directed and facilitated mesenchymal cell migration away from explants. Cells were aligned parallel to grooves and migrated 3 – 5 fold faster than those on flat surfaces. Cells attached to the ridge region were able to spread from one ridge to another by bridging the groove. However, not all cells prefer aligning along groove axes; cell reaction to groove topography depends on cell type. Rajnicek *et al.* (Rajnicek *et al.*, 1997) cultured central nerve system neurons (embryonic *Xenopus* spinal cord and embryonic rat hippocampus neurons) on quartz surfaces patterned with regular grooves (14 – 1100 nm in depth; 1, 2, and 4  $\mu\text{m}$  in width, 1  $\mu\text{m}$  spacing). The preferred direction of neurite spreading depended on cell type and dimension of the groove. Spinal neurons extended their neurites along grooves, while hippocampus neurons extended their neurites perpendicular to shallow, narrow grooves and parallel to deep, wide ones. Similarly, Webb *et al.* (Webb *et al.*, 1995) cultured oligodendrocyte progenitors, rat optic nerve astrocytes, rat hippocampal and cerebellar neurons on quartz substrates patterned with regular and irregular 1 – 4  $\mu\text{m}$  wide and 0.1 – 1.2  $\mu\text{m}$  deep grooves and 0.13 – 8  $\mu\text{m}$  ridges coated with 0.01% poly-D-lysine. When cultured on the surface grated with ~100 nm wide and 100 – 400 nm deep grooves and ridges, hippocampal and cerebellar granule cell neurons extended their neurites perpendicular to the grooves.

Cells cultured on substrates patterned with cellular and subcellular scale topography were also reported to synthesize more cell adhesion molecules (e.g., fibronectin (Fn)) than those cultured on flat surfaces. For example, Chou *et al.* (Chou *et al.*, 1995) found that human fibroblasts secreted 2-fold more ECM Fn when cultured on surfaces patterned with V-shaped grooves (3  $\mu\text{m}$  in depth, 6  $\mu\text{m}$  in width, and 10  $\mu\text{m}$  in spacing). Manwaring *et al.* (Manwaring *et al.*, 2004) studied rat meningeal cell alignment and ECM protein distribution while cultured on Fn (20  $\mu\text{g}/\text{ml}$ ) coated polystyrene surfaces patterned with irregular grooves with average roughness ranging from 50 nm to 1.6  $\mu\text{m}$ . Nanometer-scale groove topography affected both meningeal cell alignment and the alignment of cell-deposited ECM; the alignment increased with increasing surface roughness.

Cellular and subcellular scale topography affects cell adhesion on substrates, and the influence depends on shape of pattern (e.g., grooves, pits) and cell types. For example, groove topography enhanced human corneal epithelial cell adhesion. Karuri *et al.* (Karuri *et al.*, 2004) seeded SV40 human corneal epithelial cells on silicon surfaces patterned with 400 – 4000 nm wide grooves and incubated cells for 24 hours. Cells attached to silicon substrates were then transferred to a flow chamber, in which cells were exposed to different levels of shear stress. It was found that cells were most adherent to surfaces patterned with smaller features; there were more cells attached to surfaces patterned with 400 nm grooves compared to surfaces patterned with grooves larger than 400 nm when cells were subjected to the same shear force. Cukierman *et al.* (Cukierman *et al.*, 2001) compared human foreskin fibroblast morphology, migration, and adhesion when cultured on 3D ECM deposited by NIH-3T3 fibroblasts with those of cells cultured on the same substrate, but mechanically compressed into 2D. In this experiment, the composition and nano-scale fibrillous topography of 3D ECM is the same as 2D ECM; the only differences between these two substrates are the reduction of thickness from  $\sim 5 \mu\text{m}$  to  $< 1 \mu\text{m}$ , and the increase in local ECM concentration. Cell adhesion on 3D ECM was 10 fold higher than on 2D ECM 10 minutes after plating; the elongation of cells on 3D ECM was 3 fold higher than on 2D ECM 5 hours after plating. Interestingly, the difference in cell elongation disappeared after 18 hours. The migration of cells on 3D ECM was slightly slower than on 2D ECM. Kidambi *et al.* (Kidambi *et al.*, 2007) cultured 3T3 fibroblasts, Hela cells, and primary hepatocytes on surfaces of PDMS substrates patterned with micro-well arrays (1.25 – 9  $\mu\text{m}$  in diameter, 2.5  $\mu\text{m}$  in depth, and 18  $\mu\text{m}$  well center to center distance) coated with polyelectrolyte multilayers (10 layers of sulfonated poly(styrene)/poly-(diallyldimethylammonium chloride)). Micron-well topography was found to inhibit cell attachment. The number of cells adherent to patterned surfaces was lower than that to smooth surfaces. The attached cell number decreased with increase of well diameters.

Cytoskeletal organization and adhesion to substrate alter the way in which cells sense and respond to the environment, and hence affect cell proliferation and differentiation (Ingber, 1997). Rajnicek *et al.* (Rajnicek *et al.*, 1997) found that neurite growth of central nerve system neurons (embryonic *Xenopus* spinal cord and embryonic rat hippocampus neurons) was enhanced by groove patterns, and proliferation rate was greater when cells were orientated in a preferred direction. Green *et al.* (Green *et al.*, 1994) studied the growth rate of human abdomen fibroblasts (CCD-969sk) cultured on silicone surfaces patterned with 2, 5, or 10  $\mu\text{m}$  rectangular pit or pillar arrays for up to 12 days. Cells were observed to be more sensitive to small size topography (i.e. 2 and 5  $\mu\text{m}$  features) instead of 10  $\mu\text{m}$  pits or pillars. 2 and 5  $\mu\text{m}$  pillar features enhanced fibroblast proliferation as compared with the same size

pit feature and flat surfaces. Dalby *et al.* (Dalby et al., 2007) cultured human mesenchymal stem cells (MSCs) and osteoprogenitors on polymethylmethacrylate (PMMA) embossed with 120 nm diameter, 100 nm depth, and 300 nm center to center spacing pits arranged as a square array, hexagonal array, or random (with different randomness) array for 21 or 28 days. Both osteoprogenitors and MSCs exhibited bipolar morphology on planar surface, and formed dense bone nodule-like aggregates on substrates patterned with random pit array topography. Osteoprogenitors on surfaces patterned with mild random pit arrays (a few pits slightly out of alignment) also expressed raised levels of bone-specific extracellular matrix proteins: osteopontin and osteocalcin. MSCs on surfaces with mild random pit arrays exhibited osteogenic gene up-regulation (11 out of 101 genes tested). Huang *et al.* (Huang et al., 2006) grew murine myoblasts on poly(dimethylsiloxane) (PDMS) surfaces patterned with grooves 10  $\mu\text{m}$  wide, 10  $\mu\text{m}$  apart, and 2.8  $\mu\text{m}$  deep, or poly(L-lactide) (PLLA) scaffolds with either well-aligned or randomly arranged 500 nm wide fibers. Both micron-scale grooves and nanofibers inhibited cell proliferation over the first 2 days in culture. 10  $\mu\text{m}$  groove topography promoted myotube elongation by 40%, while 500 nm nanofibers enhanced myotube length by 180% after 7 days. The inhibition of cell proliferation during early culture and the promotion of myotube assembly in late culture suggested that micropatterned surfaces may enhance cell cycle exit of myoblasts and differentiation into myotubes, and that myoblasts were more sensitive to nanometer scale topography than micron-scale topography. The reduction in cell proliferation by culturing on surfaces patterned with subcellular scale topography was also observed by Yim *et al.* (Yim et al., 2005). They cultured bovine pulmonary artery smooth muscle cells (SMC) on poly(methyl methacrylate) (PMMA) and poly(dimethylsiloxane) (PDMS) surfaces patterned with 700 nm wide and 350 nm deep grooves and found that SMCs cultured on patterned surfaces incorporated significantly lower BrdU than cells cultured on flat surfaces during 4 hours of incubation. Den Braber *et al.* (Den Braber et al., 1995) cultured fibroblasts from ventral skin on PDMS substrates patterned grooves 2 – 10  $\mu\text{m}$  wide, 2 – 10  $\mu\text{m}$  spaced, and 0.5  $\mu\text{m}$  deep grooves. No effect of surface topography on cell proliferation was observed. These observations suggest that the effect of subcellular scale topography on cell behavior is highly dependant on cell type, shape and size of the pattern, and possibly the physical and chemical properties of the substrate material.

#### 4.2 Tissue subunits (submillimeter) scale topography

Subunit scale topography has also been found to affect cell morphology, adhesion, proliferation, and differentiation. However, compared with cellular and subcellular scale topography, the effect of subunit scale topography is more subtle. Dunn *et al.* (Dunn&Heath, 1976) cultured chick embryonic heart fibroblasts on the surface of cylindrical fibers with diameters ranging from 50 to 350  $\mu\text{m}$ . After 24 hours of cultivation, it was found that cell nuclei preferred to orient along the fiber axis, and the shape of aligned cell nuclei are related to fiber diameter: the smaller the diameter, the higher the axis width to cross axis width ratio. However, the effect of cylindrical topography on cell nuclei alignment disappeared when fiber diameter was bigger than 200  $\mu\text{m}$ . Brunette et al. (Brunette et al., 1983) studied outgrowth of human gingival explants on a titanium surface etched with trapezoid shape grooves (groove upper width 130  $\mu\text{m}$  and lower width 60  $\mu\text{m}$ , ridge width 10  $\mu\text{m}$ ). The direction of outgrowth was strongly guided by the grooves. Interestingly, cells preferred to reside inside grooves instead of on top of ridges, which might be due to the width of ridges

being much smaller than the width of grooves (10  $\mu\text{m}$  vs. 130  $\mu\text{m}$ ). The above studies suggested that subunit scale grooves might also provide guidance for cell migration; however, this may occur through different mechanisms than for cells aligned on surfaces patterned with submicron to nanometer scale grooves. In another study, Dunn *et al.* (Dunn&Heath, 1976) cultivated chick heart ventricle explants on surfaces of prisms with different ridge angles (i.e. 179°, 178°, 176°, 172°, 166° and 148°). It was found that abrupt change in surface orientation inhibited cell migration or changed the cell migration direction from perpendicular to the ridge to either parallel or away from the ridge; ridges with angles less than 166° inhibited cells from crossing ridges. Further investigation of microfilament arrangement inside of cells spanned across ridges suggested that the majority of microfilaments terminated when they encountered a ridge, and a new set microfilaments formed at the other side of the ridge, oriented in a completely different direction. Mata *et al.* (Mata et al., 2002) investigated human connective tissue progenitor cell spreading and colony formation on a PDMS substrate patterned with C-shape microgrooves (11  $\mu\text{m}$  deep, 45  $\mu\text{m}$  wide, separated by 5  $\mu\text{m}$  wide ridge). Cells were cultured for 9 days, and the size, shape, and cell density of cell colonies were studied. Colony area of cells grown on patterned surfaces was half the average size as that of cells on flat surfaces; however, the cell density was two times higher than on flat surfaces. The groove topography affected progenitor cell colony alignment and elongation; most cell colonies extended and spread within and along the grooves. SEM images also showed that cells located at the curvy bottom of the groove didn't attach conformally to the concave surface; instead they spanned across the concave bottom. Mrksich *et al.* (Mrksich, 2000) fabricated a polyurethane substrate patterned with V-shape grooves (25 or 50  $\mu\text{m}$  in width, 25 or 50  $\mu\text{m}$  in spacing). The groove region was coated with protein adhesive self-assembled monolayers (SAM), and the ridge region was coated with non-adhesive SAMs, or vice versa. Fn was then adsorbed to the surfaces, and bovine capillary endothelial (BCE) cells were seeded and cultured for 3 days. Cells were found only to attach to Fn adsorbed regions. SEM images of cell spreading suggested that cells located in grooves were more elongated, less spread, and had more distinctive protrusions than those located on plateau ridges. Similar to what was found when culturing human connective tissue progenitor cells inside 45  $\mu\text{m}$  wide C-shape grooves, BCE didn't attach conformally to sharp V-shape bottoms of the grooves. Instead, they spanned across them. In general, the submillimeter scale convex topography, such as the surface of a cylindrical fiber, or a surface of a prism, prevents cell migrating in a direction tangential to a curvy surface or perpendicular to a ridge; the concave topography, such as a C-shape, U-shape, or V-shape groove, induces cells to take a "short-cut" by spanning across the bottom of grooves instead of spreading conformally to the surface. Concave submillimeter topography restricts cell spreading, as cells located inside of grooves spread slower than cells on plateau ridges.

Effect of subunit scale topography on cell proliferation and differentiation has also been studied, and in general it has been found that subunit scale topography has no or very little effect on cell proliferation and differentiation. Mata *et al.* (Mata et al., 2002) cultured human connective tissue progenitor cells on PDMS substrates patterned with C-shape microgrooves (11  $\mu\text{m}$  deep, 45  $\mu\text{m}$  wide, separated by 5  $\mu\text{m}$  wide ridge) for 9 days; cells were stained for alkaline phosphatase (ALP) afterwards. The ALP staining suggested the microgroove topography did not affect the differentiation of progenitor cells into an osteoblastic phenotype. Lack of effect of substrate surface topography on cell differentiation was also



observed by Charest *et al.* (Charest et al., 2007). In their study, primary and C2C12 myoblasts were grown on surfaces of polycarbonate substrates patterned with 5 – 75  $\mu\text{m}$  wide and 5  $\mu\text{m}$  deep groove or pit arrays, and covalently coated with fibronectin. The level of sarcomeric myosin expression (marker of myogenic differentiation) was examined 50 hours after seeding for primary myoblasts and 102 hours after seeding for C2C12 myoblasts. Surface topography had no effect on sarcomeric myosin expression and cell density. The lack of effect of sub-millimeter scale topography on cell proliferation and differentiation may be due to the fact that proliferation and cell differentiation is only sensitive to nanometer to several micron scale topography, but not topographies in ten- to hundred-micron scales as mentioned in previous section (section 4.1). However, not all cell types are insensitive to ten- to hundred-micron scale topography; thus, the modulation of cell phenotype by surface topography may be cell type specific. For example, Pins *et al.* (Pins et al., 2000) cultivated human epidermal keratinocytes on type I collagen membranes patterned with sub-millimeter scale channels (40 to 310  $\mu\text{m}$  wide), which presented a similar topography as the invaginations found in native skin basal lamina. Cells grown on patterned substrates were shown to form differentiated and stratified epidermis. Zinger *et al.* (Zinger et al., 2005) grew MG63 osteoblast-like cells on titanium substrates patterned with both micron-scale cavities 100, 30 and 10  $\mu\text{m}$  in diameter and sub-micron-scale roughness ( $R_a = 0.7 \mu\text{m}$ ).  $\text{PGE}_2$  levels of cells were dependent on dimensions of micron-scale cavities. 100  $\mu\text{m}$  cavities enhanced osteoblast growth, while sub-micron-scale roughness induced cell differentiation and TGF- $\beta$ 1 production. Liao *et al.* (Liao et al., 2003) cultivated neonatal rat osteoblasts on PDMS substrates patterned with pyramid arrays (23  $\mu\text{m}$  in height and a square base with the length of each side being 33  $\mu\text{m}$ ). The patterned PDMS substrates were either exposed to oxygen plasma to increase surface hydrophilicity, or left untreated. The pyramid topography enhanced osteoblast differentiation. Cells grown on hydrophilic patterned substrates formed the most mineralized and alkaline phosphatase (ALP) positive nodules and expressed the highest ALP activities.

## 5. Theories of mechanisms

In vivo, cells grow on or inside ECM; the molecular composition, mechanical properties, and topography of ECM affect cell behavior (Reviewed by (Geiger et al., 2001)). Most adherent cells' adhesion to ECM is mediated by integrins, which are a family of transmembrane proteins responsible for signal transduction between ECM and cytoskeleton (Reviewed by (Roskelley et al., 1995) (Clark&Brugge, 1995)). Integrins interact with the actin cytoskeleton at the cell interior (Geiger et al., 2001). Cell proliferation and differentiation is a synergic response to growth factors and adhesive cues, where cell adhesion is usually mediated by integrins. The topography and morphology of cell culture substrates might affect cell adhesion ligand distribution and local concentration; the manner of cell surface receptor (integrin) interaction with ligands (3D configuration); the expression and function of cell adhesion integrins; spatial distribution of cells, which might affect cell-cell contacts and signaling; local mechanical stress, etc., all of which might eventually affect cell phenotype. Teixeira *et al.* (Teixeira et al., 2003) reported that a higher percentage of human corneal epithelial cells elongated along micron-scale grooves when cultured in serum containing medium than serum-free medium on surfaces of patterned silicon oxide. As serum contains cell adhesion proteins which can adsorb to cell culture surfaces prior to cell adhesion, this

observation suggests that surface topography affects the distribution of cell adhesion proteins (ligands) and their local concentration. Stevens *et al.* (Stevens&George, 2005) postulated that nanoscale features, such as micropores, microfibers and nanofibers, may affect the adsorption, conformation, and local distribution of integrin binding proteins, changing the availability and local concentration for interacting with integrins. The presence of surface topography might increase local ligand concentration and lead to clustering of integrin, in turn activating focal adhesion kinase, which is a prerequisite process for cell migration (Kornberg *et al.*, 1991, Sieg *et al.*, 1999). For example, it was reported that HepG2 cells formed membrane projections and focal adhesions in the middle of the cell ventral surface when cells were cultured on poly(glycolic-co-lactic)acid (PGLA) surfaces patterned with 0.92 to 3.68  $\mu\text{m}$  pores; meanwhile no membrane projections and focal adhesions were observed when cells were cultured on flat PGLA surfaces (Ranucci&Moghe, 2001). Subcellular scale pores might locally create a reservoir of cell culture medium containing high concentration of adhesion ligands, hence inducing the formation of focal adhesions in the middle of cells instead of at the cell periphery. In addition, the formation of membrane projections suggested the possible non-homogenous distribution of adhesion ligands on the patterned surface, which may require cells to generate protrusions to reach out to places having higher ligand concentration. Interestingly, similar size micro-pillar topography was reported to inhibit the formation of focal contacts. Lim *et al.* (Lim *et al.*, 2004) cultured retinal pigment epithelial cells on polydimethylsiloxane (PDMS) substrates patterned with 5  $\mu\text{m}$  in diameter and 5  $\mu\text{m}$  in spacing pillar arrays. The focal contact formation and actin filament assembly were interrupted by pillars. The subcellular scale topology might also increase the scaffold surface area, which in turn increases the total amount of integrin adsorption on the surface of scaffolds. On the other hand, subcellular topology likely modulates the interfacial forces that guide the cytoskeletal organization (Stevens&George, 2005).

Substrate surface topography affects cell morphology. One of the most well-known phenomena, described extensively above, is contact guidance: cells orient and elongate themselves parallel to instead of perpendicular to groove or cylindrical fiber axes. The smallest feature reported to induce contact guidance is 70 nm wide ridges (Teixeira *et al.*, 2003). It has been proposed that actin microfilaments (Dunn&Heath, 1976, Dunn&Brown, 1986, Heidi Au *et al.*, 2007), focal contacts (Ohara&Buck, 1979), and microtubules (Oakley&Brunette, 1993) are vital for cell adhesion. Cells spreading on grooved substrates develop cytoskeletal polarity before orienting themselves, suggesting alignment of either microtubules, microfilaments, focal contacts, or all of the above, leading to cell alignment (Oakley&Brunette, 1993). Focal adhesion and actin filament alignment along micron-scale grooves and ridges was observed in fibroblasts (Den Braber *et al.*, 1995). Actin filament assembly was found to be critical for orientation and elongation of cardiomyocytes along abrasions, as cell alignment disappeared when actin polymerization was inhibited (Heidi Au *et al.*, 2007). It was postulated that the tension generated by actin stress fibers is necessary for the focal adhesion formation (Chrzanowska-Wodnicka&Burridge, 1996); in other words, the alignment of microfilaments leads to the orientation of focal contacts. However, fibroblasts have been reported to form aligned microtubules first, followed by forming aligned focal contacts and then well-aligned actin filaments. Interestingly, microtubules preferred to concentrate and align inside grooves, while focal contacts and actin filaments formed and concentrated on tops of ridges (Oakley&Brunette, 1993). Another possible mechanism of forming aligned focal contacts along ridges may be physical

restriction. A focal contact is oval shaped, 2-5  $\mu\text{m}$  in its major axis (Geiger et al., 2001), and 250 – 500 nm in its minor axis (Ohara&Buck, 1979), suggesting that a 2-5  $\mu\text{m}$  wide ridge is required for focal contact formation in the direction perpendicular to the ridge. If a ridge is narrower than 2-5  $\mu\text{m}$ , a focal contact must orient itself parallel to the ridge to be able to fit, which causes cells to orient in the direction along ridges. This assumption is supported by some observations; for example, the percentage of human corneal epithelial cell aligned along ridges decreased when the width of ridges exceeded 2  $\mu\text{m}$  (Teixeira et al., 2003).

Other than groove and ridge topography, cylindrical fibers have also been found to control cell orientation: cells preferred elongating and extending along the long axis of a fiber rather than bending around a fiber (Dunn&Heath, 1976). It was postulated that contact guidance on cylindrical fibers and the resistance of cells to bend around a curved surface might be due to the fact that straight actin filaments are not able to assemble in a bent state (Dunn&Heath, 1976, Dunn, 1991, Rovensky&Samoilov, 1994, Rovensky Yu&Samoilov, 1994). This theory might also explain the phenomenon of cells preferring to span across concave or discontinuous surface features rather than spreading conformally on substrates. For example, Mata *et al.* (Mata et al., 2002) found that when cells were cultured on a PDMS surface patterned with C-shape microgrooves (11  $\mu\text{m}$  deep, 45  $\mu\text{m}$  wide, separated by 5  $\mu\text{m}$  wide ridges), cells located at the curved bottom of the groove spanned across the bottom. Rat liver epithelial IAR cells and fetal bovine trachea epithelial FBT cells were also found to resist bending around a cylindrical surface (12-13 or 25  $\mu\text{m}$  radii), instead of elongating along the axis (Rovensky Yu&Samoilov, 1994). SEM of cross-section of human corneal epithelial cells attached on a patterned silicon oxide surface suggested that lamellipodia of epithelial cells were not able to adhere to the bottom of 330 nm wide, 150 nm and 600 nm deep grooves, but spanned across grooves (Teixeira et al., 2003). Actin filament elongation and extension might be temporally interrupted or inhibited in circumstances where continuity of the actin filament may be disrupted by abrupt bending of the cytoplasm. However, some research suggests that formation and alignment of actin filaments and focal contacts might not be the driving force for cell contact guidance on patterned surfaces for some cell types. For example, Webb *et al.* (Webb et al., 1995) observed high alignment of oligodendrocytes and oligodendrocyte-type 2 astrocyte progenitors on surfaces patterned with submicron size grooves; however, no high-order F-actin cytoskeletal networks were observed. On the other hand, extensive organization of F-actin into stressed fibers and cables was detected among aligned astrocytes. The presence of surface topography might also create a physical barrier for cell-cell contact, or restrict available spreading area for cells, which then influences cell morphology. Direct cell-cell contact has been found to promote cell proliferation; for example, smooth muscle cells or endothelial cells contacted with one or more neighbor cells have significantly higher growth rates than single cells without contacts (Nelson&Chen, 2002).

The alteration of cell morphology was reported to affect cell proliferation and phenotype. For instance, the commitment of human mesenchymal stem cells (hMSCs) to adipocyte or osteoblast phenotype was regulated by cell shape: the widely spread and flattened hMSCs underwent osteogenesis, while round and unspread hMSCs underwent adipogenesis (Mcbeath et al., 2004). Folkman *et al.* (Folkman&Moscona, 1978) found that the shape of mammalian cells (i.e. bovine endothelial cells, WI-38 human fetal lung fibroblasts, and A-31 cells) is tightly coupled to DNA synthesis. Extremely flat shaped cells incorporate ~ 30 fold more  $^3\text{H}$ -thymidine than spheroidal conformation cells, suggesting much more active DNA synthesis of extensively spread cells. However, in this paper cell shape was modulated by

varying the substrate adhesiveness. The spheroidal cells had much lower adhesion to surfaces than flat shape cells, therefore, it was hard to uncouple the effects of cell shape and adhesion on DNA synthesis. Cukierman *et al.* (Cukierman et al., 2001) also observed the enhancement of BrdU incorporation (one of characteristics for S-phase cells) among most elongated fibroblasts, which were cultured on a 3D ECM deposited by NIH-3T3 fibroblasts. Furthermore, they found that the cell-matrix adhesion mechanism was affected by the substrate z dimensional topography. The overlapping of the focal and fibrillar adhesions was observed among cells cultured on a 3D ECM, whereas focal and fibrillar adhesions were found presenting at different locations on cell membrane when cultured on a 2D ECM with the same composition except the lack of z dimension. The focal adhesions anchor actin filaments and mediate strong adhesion of cells to the matrix; where fibrillar adhesions are associated with ECM fibrils and responsible for fibronectin generation (reviewed by (Geiger et al., 2001)). Narrowed integrin usage (i.e. involvement in only adhesion rather than adhesion and spreading, as observed on 2D surfaces) among fibroblasts cultured on 3D substrates was also observed, and the sensing of and reaction to z dimensional topography was  $\alpha 5$  integrin dependent (Cukierman et al., 2001). Wang *et al.* (Wang et al., 1998) reported a bidirectional cross-modulation of  $\beta$ -1 integrin and epidermal growth factor receptor signaling through mitogen activated protein kinase pathway in human mammary epithelial cells when cultured in 3D Matrigel™ (basement membrane from Englebreth-Holm-Swarm tumors), which didn't occur in 2D cultures. The above observations suggest that in 3D culture cell surface integrins such as  $\beta$ -1 and  $\alpha$ -5 have different function or regulate different cellular processes compared with cells cultured on a 2D substrate. It was also postulated that surface topography might lead to local restriction or redistribution of cell membrane proteins such as ion channels, which might cause cytoskeletal reorganization, or vice versa. The change of cytoskeleton was also reported to be able to regulate ion channel distribution on the cell surface; Levina *et al.* (Levina et al., 1994) found that the disruption of cortical cytoskeleton in the growing tip of the oomycete affected ion channel distribution.

Reaction of cells to surface topography is cell type dependent. This is possibly related to the fact that *in vivo* different types of cells are exposed to different 3D environments. For example, epithelial cells are often highly polarized and in direct contact with 3D basement membrane via their basolateral sides, while fibroblasts often found in connective tissues are surrounded by 3D ECM, and adapt to a specific 3D matrix. When cultured *in vitro* on patterned surface with similar 3D patterns as native ECM, cells might react as *in vivo*. In the *Xenopus* spinal cord, sensory ganglion neurons extend along longitudinally aligned Rohon-Beard neurons and aligned longitudinal channels ( $\sim 0.6 \mu\text{m}$  to  $3 \mu\text{m}$  wide) sandwiched between Rohon-Beard neurons and neighboring neuroepithelial cells (Nordlander&Singer, 1982). In hippocampus, neurites often exhibit perpendicular contact guidance on parallel arrays of pre-existing neurites (Hekmat et al., 1989). When cultured *in vitro* on a quartz surface patterned with grooves (14 - 1100 nm in depth; 1, 2, and 4  $\mu\text{m}$  in width, 1  $\mu\text{m}$  spacing), *Xenopus* spinal cord neurons extended their neurites along grooves, while hippocampus neurons extended their neurites perpendicular to shallow, narrow grooves (Rajnicek et al., 1997). *In vivo*, the diameter of a 7-day-old rat optic nerve axon is approximately  $0.19 \pm 0.5 \mu\text{m}$  in diameter (Webb et al., 1995), and *in vitro* it was observed that rat optic nerve astrocytes aligned along  $\sim 1 \mu\text{m}$  wide and  $\sim 1 \mu\text{m}$  deep grooves. Meanwhile, it was also found that cells became less sensitive to groove topography when the size of



groove features increased to several microns, which supports the theory that cells would be most sensitive to substrate topography having the size close to *in vivo* features.

Surface topography might also play a role in confining cell movement and migration, and delaying cell spreading. For example, Teixeira *et al.* (Teixeira et al., 2003) utilized time-lapse microscopy to plot human corneal epithelial cell centroid trajectories on silicon oxide surfaces patterned with 400 nm deep grooves over a 10 hour period. It was also found that centroids of cells on patterned surface were more stationary compared with cells on flat surfaces. The intestinal crypt-like well topography (50  $\mu\text{m}$  in diameter and 120  $\mu\text{m}$  in depth) was found to delay intestinal epithelial Caco-2 cell spreading for up to 2 days (Wang et al., 2009).

## 6. Conclusions

ECMs of native tissues possess unique, intricate, and often fractal topography ranging from submillimeter to nanometer scale. In the native state, cells are surrounded or in direct contact with 3D matrix, which guides cell migration, modulates cell adhesion, alters cytoskeletal organization, and affects cell phenotype. In vitro studies have documented that nanometer to submillimeter scale biomimetic topographical features influenced cell behavior, suggesting that topography of ECM plays an important role in regulating cell behavior, such as cell morphology, alignment, adhesion, migration, proliferation, and differentiation. The influence of topological cues depends on cell type, shape, and size of topographical feature; the more biomimetic topography induced more *in vivo* like cell phenotype. Relatively speaking, the majority of studies have been done using synthetic materials as cell culture scaffolds, focusing on simple topographical features (e.g. grooves and ridges) with sizes in single cell or subcellular scale (nanometer to tens micron) range and short periods of cultivation. In order to fully understand the role of ECM topography on cellular behavior and tissue function, chemically, mechanically, and physiologically more biomimetic cell culture substrates need to be fabricated. Information pertaining to the influence of topography on cell behavior will benefit rational design of tissue engineering scaffolds and *in vitro* cell model development.

## 7. References

- Abrams, G., A. et al. (2003). Ultrastructural basement membrane topography of the bladder epithelium. *Urological Research*, Vol.31, No.5, 341-346, 0300-5623
- Abrams, G. A. et al. (2000). Nanoscale topography of the basement membrane underlying the corneal epithelium of the rhesus macaque. *Cell and Tissue Research*, Vol.299, No.1, 39-46, 0302-766X
- Badylak, S. F. (2004). Xenogeneic extracellular matrix as a scaffold for tissue reconstruction. *Transplant immunology*, Vol.12, No.3-4, 367-377, 0966-3274
- Bettinger, C. J. et al. (2009). Engineering substrate topography at the micro- and nanoscale to control cell function. *Angewandte Chemie (International ed. in English)*, Vol.48, No.30, 5406-5415, 1433-7851
- Brunette, D. M. et al. (1983). Grooved titanium surfaces orient growth and migration of cells from human gingival explants. *Journal of Dental Research*, Vol.62, No.10, 1045-1048, 0022-0345
- Butcher, J. T. & Nerem, R. M. (2004). Porcine aortic valve interstitial cells in three-dimensional culture: Comparison of phenotype with aortic smooth muscle cells. *The Journal of Heart Valve Disease*, Vol.13, No.3, 478-486, 0966-8519

- Charest, J. L. et al. (2007). Myoblast alignment and differentiation on cell culture substrates with microscale topography and model chemistries. *Biomaterials*, Vol.28, No.13, 2202-2210, 0142-9612
- Choquet, D. et al. (1997). Extracellular matrix rigidity causes strengthening of integrin-cytoskeleton linkages. *Cell*, Vol.88, No.1, 39-48, 0092-8674
- Chou, L. et al. (1995). Substratum surface topography alters cell shape and regulates fibronectin mrna level, mrna stability, secretion and assembly in human fibroblasts. *Journal of Cell Science*, Vol.108, No.4, 1563-1573, 0021-9533
- Chrzanowska-Wodnicka, M.&Burridge, K. (1996). Rho-stimulated contractility drives the formation of stress fibers and focal adhesions. *The Journal of Cell Biology*, Vol.133, No.6, 1403-1415, 0021-9525
- Clark, E.&Brugge, J. (1995). Integrins and signal transduction pathways: The road taken. *Science*, Vol.268, No.5208, 233-239, 0193-4511
- Cook, G. et al. (2003). Exact replication of biological structures by chemical vapor deposition of silica. *Angewandte Chemie International Edition*, Vol.42, No.5, 557-559, 1521-3773
- Cukierman, E. et al. (2001). Taking cell-matrix adhesions to the third dimension. *Science*, Vol.294, No.5547, 1708-1712, 0193-4511
- Dalby, M. J. et al. (2007). The control of human mesenchymal cell differentiation using nanoscale symmetry and disorder. *Nature materials*, Vol.6, No.12, 997-1003, 1476-1122
- den Braber, E. T. et al. (1995). Effect of parallel surface microgrooves and surface energy on cell growth. *Journal of Biomedical Materials Research*, Vol.29, No.4, 511-518, 0021-9304
- Discher, D. E. et al. (2005). Tissue cells feel and respond to the stiffness of their substrate. *Science*, Vol.310, No.5751, 1139-1143, 0193-4511
- Dunn, G. A.&Heath, J. P. (1976). A new hypothesis of contact guidance in tissue cells. *Experimental Cell Research*, Vol.101, No.1, 1-14, 0014-4827
- Dunn, G. A.&Brown, A. F. (1986). Alignment of fibroblasts on grooved surfaces described by a simple geometric transformation. *Journal of Cell Science*, Vol.83, 313-340, 0021-9533
- Dunn, G. A. (1991). How do cells respond to ultrafine surface contours? *Bioessays*, Vol.13, No.10, 541-543, 0265-9247
- Flemming, R. G. et al. (1999). Effects of synthetic micro- and nano-structured surfaces on cell behavior. *Biomaterials*, Vol.20, No.6, 573-588, 0142-9612
- Folkman, J.&Moscona, A. (1978). Role of cell shape in growth control. *Nature*, Vol.273, No.5661, 345-349, 0028-0836
- Geiger, B. et al. (2001). Transmembrane crosstalk between the extracellular matrix--cytoskeleton crosstalk. *Nature reviews. Molecular cell biology*, Vol.2, No.11, 793-805, 1471-0072
- Gilbert, T. W. et al. (2006). Decellularization of tissues and organs. *Biomaterials*, Vol.27, No.19, 3675-3683, 0142-9612
- Green, A. M. et al. (1994). Fibroblast response to microtextured silicone surfaces: Texture orientation into or out of the surface. *Journal of Biomedical Materials Research*, Vol.28, No.5, 647-653, 1097-4636
- Hay, E. D. (1991). *Cell biology of extracellular matrix*, Plenum Press, 0306439514, New York
- Heidi Au, H. T. et al. (2007). Interactive effects of surface topography and pulsatile electrical field stimulation on orientation and elongation of fibroblasts and cardiomyocytes. *Biomaterials*, Vol.28, No.29, 4277-4293, 0142-9612
- Hekmat, A. et al. (1989). Small inhibitory cerebellar interneurons grow in a perpendicular orientation to granule cell neurites in culture. *Neuron*, Vol.2, No.2, 1113-1122, 0896-6273

- Hironaka, K. et al. (1993). Renal basement membranes by ultrahigh resolution scanning electron microscopy. *Kidney international*, Vol.43, No.2, 334-345, 0085-2538
- Huang, N. F. et al. (2006). Myotube assembly on nanofibrous and micropatterned polymers. *Nano letters*, Vol.6, No.3, 537-542, 1530-6984
- Ikari, Y. et al. (2000). A1-proteinase inhibitor,  $\alpha$ 1-antichymotrypsin, or  $\alpha$ 2-macroglobulin is required for vascular smooth muscle cell spreading in three-dimensional fibrin gel. *Journal of Biological Chemistry*, Vol.275, No.17, 12799-12805, 0021-9258
- Ingber, D. E. (1997). Tensegrity: The architectural basis of cellular mechanotransduction. *Annual review of physiology*, Vol.59, 575-599, 0066-4278
- Karuri, N. W. et al. (2004). Biological length scale topography enhances cell-substratum adhesion of human corneal epithelial cells. *Journal of Cell Science*, Vol.117, No.15, 3153-3164, 0021-9533
- Kawabe, T. T. et al. (1985). Variation in basement membrane topography in human thick skin. *The Anatomical Record*, Vol.211, No.2, 142-148, 1552-4892
- Kidambi, S. et al. (2007). Cell adhesion on polyelectrolyte multilayer coated polydimethylsiloxane surfaces with varying topographies. *Tissue Engineering*, Vol.13, No.8, 2105-2117, 1076-3279
- Kornberg, L. J. et al. (1991). Signal transduction by integrins: Increased protein tyrosine phosphorylation caused by clustering of beta 1 integrins. *Proceedings of the National Academy of Sciences of the United States of America*, Vol.88, No.19, 8392-8396, 0027-8424
- Lee, K. Y. & Mooney, D. J. (2001). Hydrogels for tissue engineering. *Chemical Reviews*, Vol.101, No.7, 1869-1880, 0009-2665
- Levina, N. et al. (1994). Cytoskeletal regulation of ion channel distribution in the tip-growing organism *saprolegnia ferax*. *Journal of Cell Science*, Vol.107, No.1, 127-134, 0021-9533
- Liang, D. et al. (2007). Functional electrospun nanofibrous scaffolds for biomedical applications. *Advanced Drug Delivery Reviews*, Vol.59, No.14, 1392-1412, 0169-409X
- Liao, H. et al. (2003). Response of rat osteoblast-like cells to microstructured model surfaces in vitro. *Biomaterials*, Vol.24, No.4, 649-654, 0142-9612
- Lim, J.-M. et al. (2004). Retinal pigment epithelial cell behavior is modulated by alterations in focal cell-substrate contacts. *Investigative ophthalmology & visual science*, Vol.45, No.11, 4210-4216, 0146-0404
- Manwaring, M. E. et al. (2004). Contact guidance induced organization of extracellular matrix. *Biomaterials*, Vol.25, No.17, 3631-3638, 0142-9612
- Martín-Palma, R. J. & et al. (2008). Replication of fly eyes by the conformal-evaporated-film-by-rotation technique. *Nanotechnology*, Vol.19, No.35, 355704, 0957-4484
- Mata, A. et al. (2002). Analysis of connective tissue progenitor cell behavior on polydimethylsiloxane smooth and channel micro-textures. *Biomedical Microdevices*, Vol.4, No.4, 267-275, 1387-2176
- McBeath, R. et al. (2004). Cell shape, cytoskeletal tension, and rhoa regulate stem cell lineage commitment. *Developmental Cell*, Vol.6, No.4, 483-495, 1534-5807
- Merker, H.-J. (1994). Morphology of the basement membrane. *Microscopy Research and Technique*, Vol.28, No.2, 95-124, 1097-0029
- Mikos, A. G. et al. (1993a). Preparation of poly(glycolic acid) bonded fiber structures for cell attachment and transplantation. *Journal of Biomedical Materials Research*, Vol.27, No.2, 183-189, 1097-4636
- Mikos, A. G. et al. (1993b). Laminated three-dimensional biodegradable foams for use in tissue engineering. *Biomaterials*, Vol.14, No.5, 323-330, 0142-9612

- Mikos, A. G. & Temenoff, J. S. (2000). Formation of highly porous biodegradable scaffolds for tissue engineering. *Journal of Biotechnology*, Vol.3, No.2, 0168-1656
- Mooney, D. J. et al. (1996). Novel approach to fabricate porous sponges of poly(-lactic-co-glycolic acid) without the use of organic solvents. *Biomaterials*, Vol.17, No.14, 1417-1422, 0142-9612
- Mrksich, M. (2000). A surface chemistry approach to studying cell adhesion *Chemical Society reviews*, Vol.29, 267-273, 0306-0012
- Nelson, C. M. & Chen, C. S. (2002). Cell-cell signaling by direct contact increases cell proliferation via a pi3k-dependent signal. *FEBS Letters*, Vol.514, No.2-3, 238-242, 0014-5793
- Nielson, R. et al. (2009). Microreplication and design of biological architectures using dynamic-mask multiphoton lithography. *Small*, Vol.5, No.1, 120-125, 1613-6829 (Electronic)
- Nordlander, R. H. & Singer, M. (1982). Spaces precede axons in xenopus embryonic spinal cord. *Experimental Neurology*, Vol.75, No.1, 221-228, 0014-4886
- Oakley, C. & Brunette, D. (1993). The sequence of alignment of microtubules, focal contacts and actin filaments in fibroblasts spreading on smooth and grooved titanium substrata. *Journal of Cell Science*, Vol.106, No.1, 343-354, 0021-9533
- Ohara, P. T. & Buck, R. C. (1979). Contact guidance in vitro. A light, transmission, and scanning electron microscopic study. *Experimental Cell Research*, Vol.121, No.2, 235-249, 0014-4827
- Pfluger, C. A. et al. (2010). Biocompatibility of plasma enhanced chemical vapor deposited poly(2-hydroxyethyl methacrylate) films for biomimetic replication of the intestinal basement membrane. *Biomacromolecules*, Vol.11, No.6, 1579-1584, 1525-7797
- Pins, G. D. et al. (2000). Microfabrication of an analog of the basal lamina: Biocompatible membranes with complex topographies. *The FASEB Journal*, Vol.14, No.3, 593-602, 0892-6638
- Pouyani, T. et al. (1994). Novel hydrogels of hyaluronic acid: Synthesis, surface morphology, and solid-state nmr. *Journal of the American Chemical Society*, Vol.116, No.17, 7515-7522, 0002-7863
- Rajnicek, A. et al. (1997). Contact guidance of cns neurites on grooved quartz: Influence of groove dimensions, neuronal age and cell type. *Journal of Cell Science*, Vol.110, No.23, 2905-2913, 0021-9533
- Ranucci, C. S. & Moghe, P. V. (2001). Substrate microtopography can enhance cell adhesive and migratory responsiveness to matrix ligand density. *Journal of Biomedical Materials Research*, Vol.54, No.2, 149-161, 1552-4965
- Raub, C. B. et al. (2007). Noninvasive assessment of collagen gel microstructure and mechanics using multiphoton microscopy. *Biophysical journal*, Vol.92, No.6, 2212-2222, 0006-3495
- Roskelley, C. D. et al. (1995). A hierarchy of ecm-mediated signaling regulates tissue-specific gene-expression. *Current Opinion in Cell Biology*, Vol.7, No.5, 736-747, 0955-0674
- Rovensky, Y. A. & Samoilov, V. I. (1994). Morphogenetic response of cultured normal and transformed fibroblasts, and epitheliocytes, to a cylindrical substratum surface. Possible role for the actin filament bundle pattern. *J Cell Sci*, Vol.107, No.5, 1255-1263, 0021-9533 (Print)
- Rovensky Yu, A. & Samoilov, V. I. (1994). Morphogenetic response of cultured normal and transformed fibroblasts, and epitheliocytes, to a cylindrical substratum surface. Possible role for the actin filament bundle pattern. *Journal of Cell Science*, Vol.107 No.5, 1255-1263, 0021-9533



- Sieg, D. J. et al. (1999). Required role of focal adhesion kinase (fak) for integrin-stimulated cell migration. *Journal of Cell Science*, Vol.112 No.16, 2677-2691, 0021-9533
- Sniadecki, N. J. et al. (2006). Nanotechnology for cell-substrate interactions. *Annals of Biomedical Engineering*, Vol.34, No.1, 59-74, 0090-6964
- Stevens, M. M.&George, J. H. (2005). Exploring and engineering the cell surface interface. *Science*, Vol.310, No.5751, 1135-1138, 1095-9203 (Electronic)
- Takahashi-Iwanaga, H. et al. (1999). Porosity of the epithelial basement membrane as an indicator of macrophage-enterocyte interaction in the intestinal mucosa. *Archives of histology and cytology*, Vol.62, No.5, 471-481, 0914-9465
- Takeuchi, T.&Gonda, T. (2004). Distribution of the pores of epithelial basement membrane in the rat small intestine. *The Journal of veterinary medical science*, Vol.66, No.6, 695-700, 0916-7250
- Teixeira, A. I. et al. (2003). Epithelial contact guidance on well-defined micro- and nanostructured substrates. *Journal of Cell Science*, Vol.116, No.10, 1881-1892, 0021-9533
- Tibbitt, M. W.&Anseth, K. S. (2009). Hydrogels as extracellular matrix mimics for 3d cell culture. *Biotechnology and bioengineering*, Vol.103, No.4, 655-663, 1097-0290
- Vercruysse, K. P. et al. (1997). Synthesis and in vitro degradation of new polyvalent hydrazide cross-linked hydrogels of hyaluronic acid. *Bioconjugate Chemistry*, Vol.8, No.5, 686-694, 1043-1802
- Wang, F. et al. (1998). Reciprocal interactions between beta1-integrin and epidermal growth factor receptor in three-dimensional basement membrane breast cultures: A different perspective in epithelial biology. *Proceedings of the National Academy of Sciences of the United States of America*, Vol.95, No.25, 14821-14826, 0027-8424
- Wang, L. et al. (2009). Influence of micro-well biomimetic topography on intestinal epithelial caco-2 cell phenotype. *Biomaterials*, Vol.30, No.36, 6825-6834, 0142-9612
- Wang, L. et al. (2010). Synergic effects of crypt-like topography and ecm proteins on intestinal cell behavior in collagen based membranes. *Biomaterials*, Vol.31, No.29, 7586-7598, 0142-9612
- Wang, Y. et al. (2005). Replication of biological organizations through a supercritical fluid route. *Chemical communications*, Vol.21, No.23, 2948-2950, 1359-7345
- Webb, A. et al. (1995). Guidance of oligodendrocytes and their progenitors by substratum topography. *Journal of Cell Science*, Vol.108, No.8, 2747-2760, 0021-9533
- Whang, K. et al. (1995). A novel method to fabricate bioabsorbable scaffolds. *Polymer*, Vol.36, 837-842, 0032-3861
- Wood, A. (1988). Contact guidance on microfabricated substrata: The response of teleost fin mesenchyme cells to repeating topographical patterns. *Journal of Cell Science*, Vol.90, No.4, 667-681, 0021-9533
- Yim, E. K. F. et al. (2005). Nanopattern-induced changes in morphology and motility of smooth muscle cells. *Biomaterials*, Vol.26, No.26, 5405-5413, 0142-9612
- Yurchenco, P. D.&Schittny, J. C. (1990). Molecular architecture of basement membranes. *FASEB Journal*, Vol.4, No.6, 1577-1590, 0892-6638
- Zinger, O. et al. (2005). Differential regulation of osteoblasts by substrate microstructural features. *Biomaterials*, Vol.26, No.14, 1837-1847, 0142-9612



### **Advances in Biomimetics**

Edited by Prof. Marko Cavrak

ISBN 978-953-307-191-6

Hard cover, 522 pages

**Publisher** InTech

**Published online** 26, April, 2011

**Published in print edition** April, 2011

The interaction between cells, tissues and biomaterial surfaces are the highlights of the book "Advances in Biomimetics". In this regard the effect of nanostructures and nanotopographies and their effect on the development of a new generation of biomaterials including advanced multifunctional scaffolds for tissue engineering are discussed. The 2 volumes contain articles that cover a wide spectrum of subject matter such as different aspects of the development of scaffolds and coatings with enhanced performance and bioactivity, including investigations of material surface-cell interactions.

### **How to reference**

In order to correctly reference this scholarly work, feel free to copy and paste the following:

Lin Wang and Rebecca L. Carrier (2011). Biomimetic Topography: Bioinspired Cell Culture Substrates and Scaffolds, *Advances in Biomimetics*, Prof. Marko Cavrak (Ed.), ISBN: 978-953-307-191-6, InTech, Available from: <http://www.intechopen.com/books/advances-in-biomimetics/biomimetic-topography-bioinspired-cell-culture-substrates-and-scaffolds>

**INTech**  
open science | open minds

### **InTech Europe**

University Campus STeP Ri  
Slavka Krautzeka 83/A  
51000 Rijeka, Croatia  
Phone: +385 (51) 770 447  
Fax: +385 (51) 686 166  
[www.intechopen.com](http://www.intechopen.com)

### **InTech China**

Unit 405, Office Block, Hotel Equatorial Shanghai  
No.65, Yan An Road (West), Shanghai, 200040, China  
中国上海市延安西路65号上海国际贵都大饭店办公楼405单元  
Phone: +86-21-62489820  
Fax: +86-21-62489821

© 2011 The Author(s). Licensee IntechOpen. This chapter is distributed under the terms of the [Creative Commons Attribution-NonCommercial-ShareAlike-3.0 License](https://creativecommons.org/licenses/by-nc-sa/3.0/), which permits use, distribution and reproduction for non-commercial purposes, provided the original is properly cited and derivative works building on this content are distributed under the same license.

IntechOpen

IntechOpen